Heliyon 9 (2023) e20662

Contents lists available at ScienceDirect

Heliyon

journal homepage: www.cell.com/heliyon

Identification of small molecules that suppress cell invasion and metastasis promoted by WASF3 activation

Jeane Silva [a,b,*], Nivin Omar [c], Vinoth Sittaramane [d], John K. Cowell [a]

[a] The Georgia Cancer Center, 1410 Laney Walker Blvd., Augusta, GA 30912, Georgia
[b] Department of Interdisciplinary Health Sciences, College of Allied Sciences, Augusta University, GA, 30912, Georgia
[c] Department of Pathology, Medical College of Georgia, Augusta University, GA, 30912, Georgia
[d] Department of Biology, Georgia Southern University, Statesboro, GA 30458, Georgia

ARTICLE INFO

Keywords:
WASF3
metastasis
In silico screen
Small molecules
MDA-MB-231
Du145
Cellular thermal shift assay
Zebrafish model of metastasis

ABSTRACT

The WASF3 gene promotes cancer cell invasion and metastasis, and genetic inactivation leads to suppression of metastasis. To identify small molecules that might interfere with WASF3 function, we performed an in silico docking study to the regulatory pocket of WASF3 using the National Cancer Institute (NCI) diversity set VI small molecule library. Compounds that showed the maximum likelihood of interaction with WASF3 were screened for their effect on cell movement in breast and prostate cancer cells, a well-established predictor of invasion and metastasis. Three hit compounds were identified that affected cell movement, and the same compounds also suppressed cell migration and invasion in vitro in both MDA-MB-231 breast cancer cells and Du145 prostate cancer cells. Using a zebrafish metastasis assay, one of these compounds, NSC670283, showed significant suppression of metastasis in vivo while not affecting cell proliferation. NSC670283 showed a consistent effect on suppression of invasion and metastasis, and cellular temperature shift assays provided support for physical interaction with WASF3. In addition, suppression of cell movement and invasion was accompanied by a decrease in actin filament polymerization. The data in this study suggest that these small molecules inhibit cancer cell invasion and metastasis, and to our knowledge, it is the first identification of a small molecule that can potentially inhibit WASF3-directed metastasis, laying the foundation for medicinal chemistry approaches to enhance the potency of the identified compounds.

1. Introduction

Metastasis is a primary reason for mortality in cancer patients, and there is extensive evidence that this particular phenotype, which develops as the tumor progresses, is genetically determined [1,2]. Genes and pathways that might be involved in this transition to an invasive phenotype have been described, including the WASF3 gene [3,4], which is an essential conduit from external stimuli to a variety of downstream effector pathways that contribute to invasion and metastasis [5–8]. Targeted knockdown of WASF3 function in highly metastatic cells leads to suppression of invasion and metastasis [9–13], and overexpressing WASF3 in non-metastatic cells increased their invasion potential [5]. These observations led to the development of a stapled peptide approach targeting essential protein-protein interactions required for WASF3 function, which suppressed invasion and metastasis [11–13]. WASF proteins have

* Corresponding author. The Georgia Cancer Center, 1410 Laney Walker Blvd., Augusta, GA 30912, Georgia.
E-mail address: jsilva@augusta.edu (J. Silva).

https://doi.org/10.1016/j.heliyon.2023.e20662
Received 7 April 2023; Received in revised form 30 September 2023; Accepted 3 October 2023
Available online 10 October 2023

been shown to bind to a complex of proteins called the WASF regulatory complex (WRC), which regulates its stability and includes NCKAP1/2, CYFIP1/2, ABI1/2, and BRK300 [14–16]. These proteins maintain the WASF3 structure in a closed, auto-inhibited conformation that prevents phospho-activation and consequent release of the *C*-terminal VCA domain that initiates actin polymerization leading to cell motility, which is an essential component of invasion [17]. Knockdown of either the NCKAP1 or CYFIP1 proteins in highly metastatic cells has been shown to destabilize the protein complex, leading to loss of WASF3 and suppression of invasion and metastasis [11,12]. Crystal structure analysis of the WRC demonstrated the importance of the WRC in maintaining the stability of the proteins and identified an essential pocket region that maintains the structure [18]. Peptidomimetics that compete for binding between proteins within the WRC lead to the disruption of this complex [11,12]. Despite the demonstration that protein mimics and stapled peptides can affect WASF3 function, to our knowledge, there have still been no small molecules identified that can suppress WASF3 function and inhibit invasion. Identifying small molecules that inhibit specific phenotypes through high throughput screening is time-consuming and expensive and depends on the availability of a convenient assay to report the phenotype [19]. Currently, invasion assays are cell-based, which do not readily lend themselves to unbiased analyses of small molecule libraries. An alternative approach is to use docking analyses in silico prediction of drug-protein interactions, which can streamline the selection of potential candidate compounds, allowing a more focused analysis of their effect on cell phenotypes [20]. This study used this approach to identify compounds that potentially interact with WASF3 through the WRC complex domain pocket. In addition, an extensive survey of in vitro invasion assays and in vivo metastasis assays in zebrafish was performed to identify a lead compound that offers a potential candidate for suppression of invasion and metastasis.

2. Experimental procedures

2.1. Cell culture

Cell lines MDA-MB-231 and Du145 were purchased from the American Type Culture Collection (ATCC, Rockville, MD). Cells were cultured in RPMI 1640 media and supplemented with 10 % fetal bovine serum (FBS) using standard cell culture conditions for human cell lines.

2.2. Molecular docking

The NCI Diversity Set VI from the DTP program was used in the docking process. Since the NCI provides only structural formulae (i.e., 2D connectivity data), these structures were converted to 3D structures using the Obgen software from the Openbabel suite [21]. Compounds from this set were then docked against the structure of the human WASF regulatory complex (PDB refcode 4N78), and the 60 compounds with the highest significant binding energies were selected for further analysis. Docking employs shortcuts, such as empirical scoring functions in place of accurate potentials and systematic phase space searches to explore the conformations of the ligand and find the optimal one. A 24*24*24 Å search box centered on the previously reported binding site of the WIRS peptide [18] recognition sequence was used, and docking was achieved using Autodock Vina software [22].

2.3. Wound-closure assay

Cells were seeded into 12-well plates at $\sim 0.3 \times 10^6$ per well. Confluent monolayers were starved overnight, and a single scratch wound was created by dragging a 20 μl plastic pipette tip across the cell surface. Cells were washed with Phosphate-Buffered Saline (PBS) once to remove cell debris and supplemented with RPMI culture media containing 2 % FBS. The area of a defined region within the scratch was measured using ImageJ software at time = 0 and again after 18 h. The extent to which the wound had closed over 18 h (motility index) was calculated and expressed as a percentage of the difference between times 0 and 18 h. Each assay was performed in 4 parallel wells, and the mean closure was calculated. Compounds being evaluated were then added into the wells at the determined concentration, and a photograph was taken after 18 h. The percentage area of the wound that was closed at the end of the experiment was determined using ImageJ software (V 1.53e). Distributed throughout the plates were wells that were treated with DMSO only. For each series of experiments, the mean closure amongst the DMSO- treated wells was calculated, and then the wound closure for drug-treated cells was expressed as a percentage of closure seen in the DMSO controls.

2.4. Migration/invasion assay

Migration and invasion assays were performed using the same protocol but with different inserts. For migration, uncoated inserts were used to evaluate the ability to migrate through pores in the membrane. For invasion assays, the Corning BioCoat Tumor Invasion System (BD Bioscience, MD) was used with an 8 μm pore size polyethylene terephthalate (PET) membrane coated with Corning Matrigel Matrix. The plate was rehydrated with warm Phosphate-Buffered Saline (PBS), 500 μL/well, at 37 °C for 2 h. After rehydration, the PBS was carefully aspirated and discarded without disturbing the membrane.

In both assays, serum-starved cells were added in the upper chamber $\sim 5 \times 10^4$ cells/0.2 mL (~50.000/per chamber), and a complete medium with 10 % FBS was used as a chemoattractant in the lower chamber. Where indicated, the individual compounds were added to the lower chamber at the specified concentration. For migration assays, the plates were then incubated at 37 °C for 24 h, and then the upper chamber was transferred into another 24-well plate containing 500 μL/well of 0.2 % crystal violet to stain migrated cells. Images were captured using a Zeiss LSM-inverted microscope, and the number of invading cells was counted using ImageJ. For

cell invasion assays, the upper chambers were transferred to another 24-well plate containing 500 μL/well of 4 μg/mL Calcein-AM fluorescence dye (BD Bioscience, MD) in Hanks' Balanced Salt Solution (HBSS) and incubated for 1 h at 37 °C. According to the manufacturer's instructions, fluorescence was measured using the SpectraMax M5 Microplate Reader with the excitation and emission wavelength 494/517 nm (Ex/Em).

2.5. Cell proliferation assays

Cells were seeded at 2.5×10^4 cells/well in a 96-well microtiter plate and exposed to individual compounds and DMSO at the determined effective concentrations. After 24, 48, and 72 h treatment, the cells were washed with PBS and incubated with PrestoBlue reagent (Invitrogen, Cat# A13261) according to the manufacturer's instructions. The changes in cell viability were detected using bottom-read fluorescence at excitation = 570 nm/emission = 610 nm for the recommended time of incubation (10 min-endpoint). The cell viability was expressed as a time course using PrestoBlue Relative Fluorescent Units (RFUs).

2.6. Western blotting

Cells were lysed in PBS containing a mixture of halt protease and phosphatase inhibitor cocktail (ThermoFisher, Cat# 78440). Then, two consecutive freeze-thaw cycles were performed, and the cell lysate was analyzed using SDS–PAGE, followed by immunoblotting using standard protocols with the respective antibodies. Briefly, after blocking with 5 % skimmed milk, membranes were probed with primary antibodies at 4 °C overnight. The membrane was washed three times and then incubated with secondary antibodies at room temperature for 1 h. Immunoreactive proteins were developed with enhanced chemiluminescence reagents (Pierce, Rockford, IL, USA). The following antibodies were used: rabbit anti-WASF3 (1:500, Cat # 2806, Cell Signaling, Danvers, MA, USA) and monoclonal mouse anti-β-actin peroxidase (1:30000, Cat # A3854, Sigma). Horseradish peroxidase-conjugated anti-rabbit was used as a secondary antibody (GE Healthcare NA934-1 ML).

2.7. Zebrafish in vivo assays

Metastasis assays were carried out essentially as described previously [23] with fluorescent cell tracker CM-DiI (Invitrogen, Carlsbad, CA, USA) labeled human metastatic cells injected into the perivitelline space of 3-day-old embryos. Metastasis was evaluated 36–48 h later using whole-mount confocal microscopy. Each compound was evaluated on four separate occasions using at least ten individual fish on each occasion (N = 40) by adding the compound at the indicated dose into the fish water in 24-well plates. Conservative estimates of metastasis were defined where at least ten cells had migrated from the injection site into the fish body. All fish were treated at the predetermined maximum tolerated dose (see text).

2.8. Immunofluorescence staining of F-actin

Coverslips were coated with poly-L-lysine for 30 min, then washed twice with deionized water and dried for approximately 1 h. MDA-MB-231 cells were grown on these coverslips for 24 h to ~80 % confluence and exposed to either DMSO or N20 (10 μM) for 18 h. Subsequently, the culture medium was removed, and cells were washed once with PBS, fixed using IC Fixation Buffer (eBioscience), and permeabilized with 0.1 % Triton X-100 in PBS for 10 min at RT. Filamentous actin (F-actin) was stained with Monoclonal anti-β-actin peroxidase (1:30,000) produced in mice (Sigma, cat# A3854 -200μL) by incubating the cells in the dark for 30 min. The wells were washed with PBS and stained for 15 min at 37 °C with 4′,6-diamidino-2-phenylindole (DAPI) to reveal cell nuclei. After 2 PBS washes, the coverslips were mounted with IMMU-MOUNT (Thermo Scientific) media and sealed. F-actin staining was observed directly using a Stellaris 5 Confocal microscope (Leica Microsystems).

2.9. Cellular thermal shift assay (CTSA)

The protocol was adopted from Jafari et al. [24]. Cells were cultured to a final density of 2×10^6 cells/ml, harvested, and distributed equally into 2 x 15 mL tubes. One tube was treated with DMSO and the other with the test compound for 1 h at 37 °C. Cells were then centrifuged in 15 mL conical tubes at 300 g at room temperature for 3 min, and the pellet was washed twice with PBS. Cells were then re-suspended in 700 μL of PBS plus protease/phosphatase inhibitors, and 100 μl from each sample was distributed evenly into seven 0.2 mL microcentrifuge tubes. Paired tubes were then placed in a thermal cycler at the required temperature for 3 min and then transferred to room temperature for another 3 min before being snap frozen on dry ice for 3 min and stored at −70 °C. Before analysis, the lysis reaction was performed through two consecutive freeze-thaw procedures. Western blot for soluble protein detection was performed as described above.

3. Results

Our objective was to screen and identify small molecules that affect WASF3-induced cell invasion. It is known that acidic phospholipids are involved in the recruitment of the WASF complex to the cell membrane [16] and that their activity is regulated by individual kinases and GTPases [17]. Recently, a consensus motif was identified that binds to a surface patch of the fully assembled WASF complex that is found in ~120 transmembrane or membrane-associated proteins [18], which is involved in the recruitment and

regulation of WASF complex activity. The crystal structure of the WASF complex with this recognition peptide has been published (PDB ref code 4N78), which seemed a more promising target site for binding by small molecules compared with either the phospholipid-binding site or the several phosphorylation sites since phospholipid binding is notoriously weak and phosphorylation is better disrupted by targeting kinases. Consequently, we used the crystal structure of the WASF regulatory complex site to identify small molecules that were predicted to interact with the WASF3 structure. The National Cancer Institute (NCI) diversity set VI, consisting of 1584 compounds, was used primarily because these molecules are generally well characterized, structurally diverse, and freely available [25]. The scoring algorithm in this in silico approach is based on molecular mechanics force fields that estimate the energy of the pose within the binding site. A low energy implies a stable system and, therefore, a likely binding interaction. From the first pass screen of this collection of compounds, we selected 60 with the highest negative binding scores for further analysis. For convenience, these are referred to as N1–N60, and their NCI identifiers are provided in Supplemental Table 1.

3.1. *Screening compounds for suppression of cell motility*

One of the most consistent indicators of in vitro cell migration/invasion in our hands [6] has been the wound-closure assay (WCA). Using a highly invasive cell line such as the MDA-MB-231 breast cancer cell line, an artificial wound is made in a confluent cell monolayer, and the ability of the cells to close that wound over 18 h was evaluated. For drug screening assays, cells treated with DMSO vehicle were compared with cells in which the individual compounds had been added. The prediction was that any compound

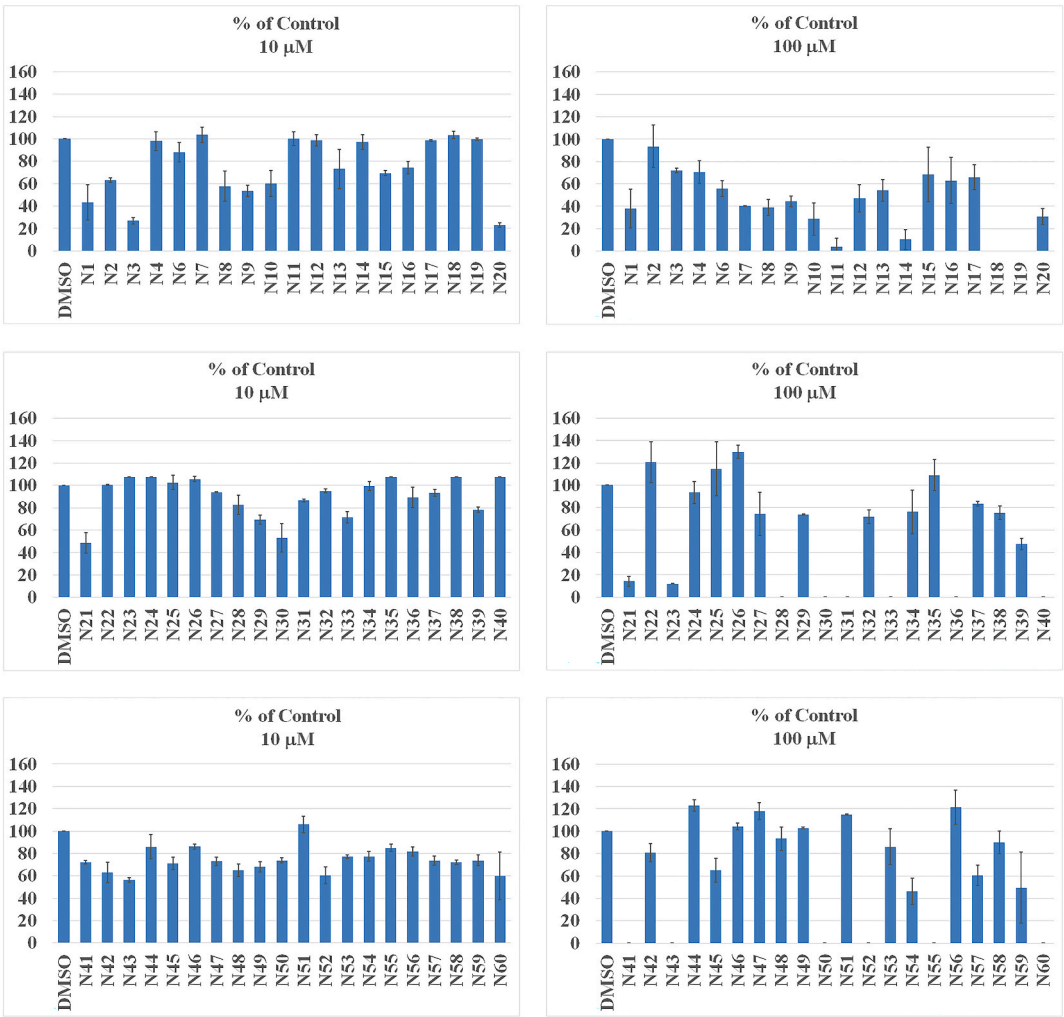

Fig. 1. Primary screen of compounds for effect on cell motility. MDA-MB-231 human breast cancer cells were seeded into 12 well plates and wounds created. Cells were then treated with each of the 60 compounds from the NCI Chemical diversity set VI at 10 μM (left) and 100 μM (right) in replicates of 4 wells. Similarly, sets of 4 wells in triplicate were treated with DMSO (N = 12). Motility is expressed as the relative percentage of wound closure after 18 h compared with the DMSO control. In cases where there is no data (mostly at the 100 μM concentration), e.g., compound N3, the compounds were toxic at the particular dose.

potentially interacting with WASF3, possibly affecting its function, would negatively affect the motility of these metastatic breast cancer cells. Cell monolayers were established in 12-well plates, and wounds were created. The cells were then washed with PBS, and the medium replaced in which the 60 compounds were included, initially at a final concentration of 10 μM. Individual compounds were assayed in batches of 20 using four different wells, and DMSO controls were included randomly in 12 different wells in different plates. After 18 h, the extent of wound closure was assessed using ImageJ (V 1.53), as we have described previously [6,10]. In each batch, the mean WC from the 12 wells treated with DMSO was calculated, and the wound closure for each of the four wells treated with compounds was expressed as a percentage of the mean DMSO control. For some of the compounds, there was evidence in the wells of cell detachment and floating debris, which indicate cell toxicity. These compounds were excluded from further analysis.

As shown in Fig. 1, several of the non-toxic compounds showed effective suppression of motility as defined by >50 % reduction in wound closure. WCAs were then repeated using the compounds at 100 μM, where toxicity was again identified for many of the compounds. These assays were once more performed using the compounds at 1 μM, where none showed comparable effectiveness (data not shown). In all, three compounds (N20, N43, and N54) showed effective suppression of motility, with two (N20 and N43) showing effectiveness at 10 μM and another (N54) at 100 μM. Examples of the WCA are shown in Supplemental Fig. 1. The molecular

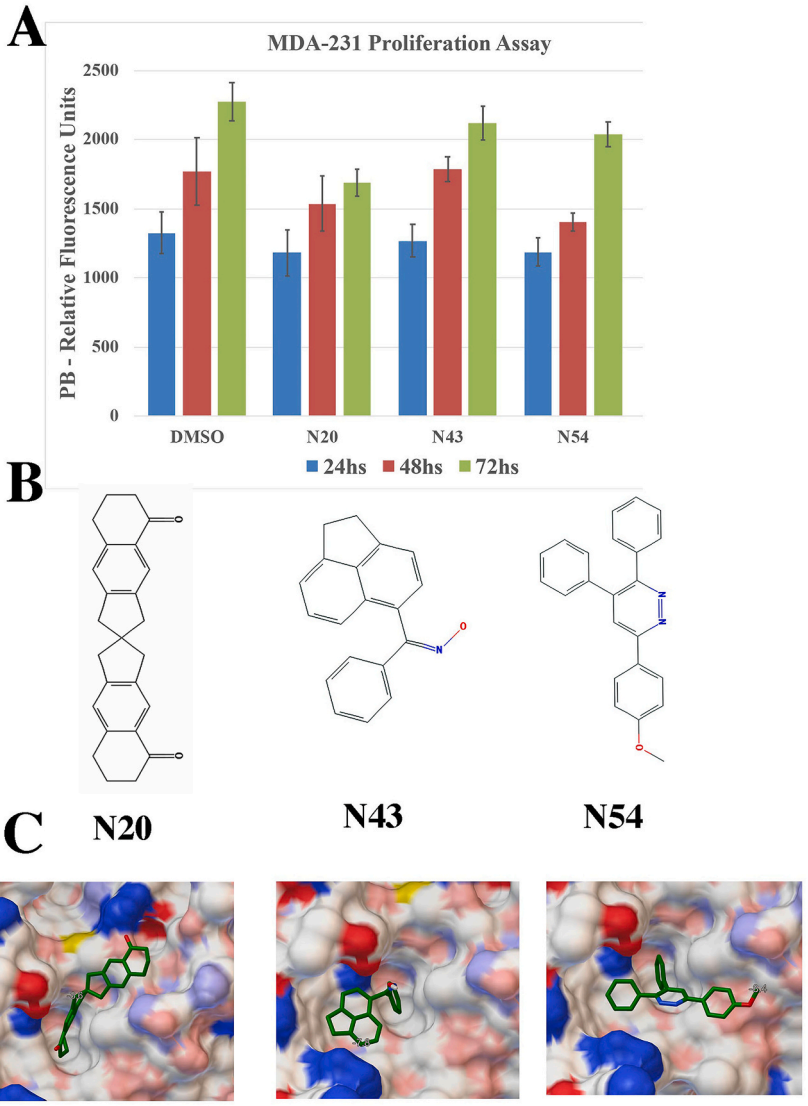

Fig. 2. Proliferation assays and docking profile. Analysis of cell proliferation over 72 h using PrestoBlue (PB) quantitation assays (N = 6) for each compound compared with the DMSO control (A). Chemical structures for the lead compounds identified as affecting motility during the wound closure assay are shown (B). Predicted docking structures for lead compounds engagement into the binding pocket for each of the three lead compounds (C). Several common features were identified where the docking output would indicate that the ligand always binds to a hydrophobic groove on the surface of the WAVE complex and that a side chain, if present, especially a phenyl side-chain, binds to the same pocket seen for the phenylalanine side-chain of the recognition motif.

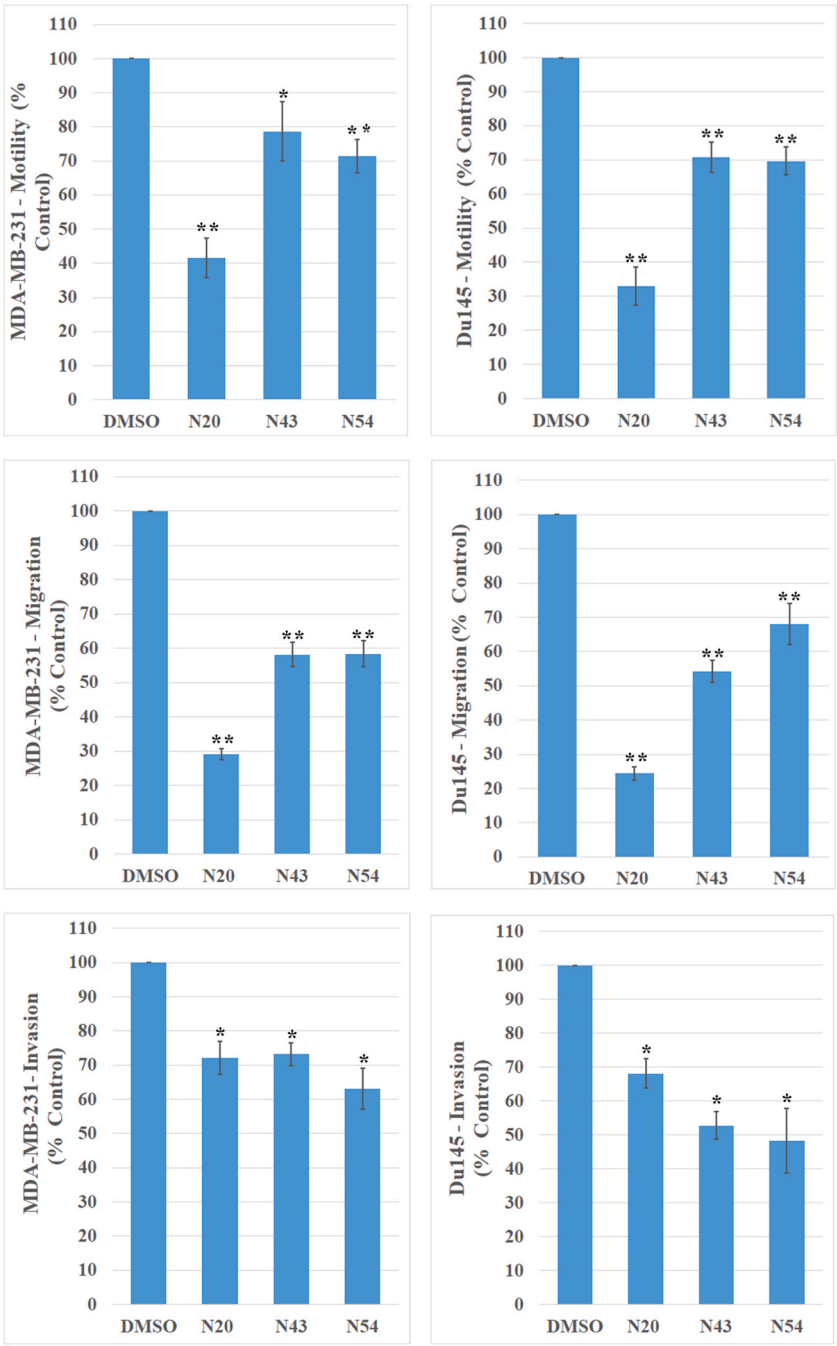

Fig. 3. Motility, Migration, and Invasion Assays. Summary of the effects of lead compounds on motility (above), migration (center), and invasion potential (below) in MDA-MB-231 cells (left panels) and Du145 cells (right panels) compared with DMSO-treated cells. Motility is defined by the relative percentage of wound closure over 18 h and represents the mean for MDA-MB-231 (n = 16) and Du145 (n = 10). Migration was determined as the number of cells that passed through the membrane pores over 18 h expressed as a percentage of that seen for DMSO-treated cells. In these studies replicates were analyzed for N20 (N = 35), N43 (N = 29) and N54 (N = 34) compared with DMSO (N = 28) for MDA-MB-231. For Du145 cells, N20 (N = 20), N43 (N = 20), and N54 (N = 14) replicates were also expressed as a percentage of the mean migration levels seen in DMSO-treated cells (N = 35). Invasion assays were quantitated using Calcein-AM fluorescence, and the values presented as a percentage of those seen for DMSO-treated cells (N = 20) calculated for N20, N43, and N54 (N = 6) in MDA-MB-231 and Du145 cells. *p = 0.01, **p = 0.001.

structures of these compounds are shown in Fig. 2, identifying a similar macrocyclic structure. Predicted docking structures for engagement of the lead compounds into the binding pocket are shown in Fig. 2C.

3.2. Effect of lead compounds on cell viability

Part of the assessment of the ability of individual drugs to affect cell migration and invasion depends on the extent to which the drug also shows cytotoxicity. Migration, however, is typically assayed over 12–24 h and is not significantly affected by cell proliferation kinetics. Given the relatively large number of compounds for cell-based assays, in the preliminary screens, we triaged those showing the excessive presence of detached cells in the supernatant at the time of the WCA analysis as an indication of toxicity. For the three lead compounds, however, we performed more detailed cell viability assays. As shown in Fig. 2, while DMSO alone has a relatively minor effect on proliferation, there was no significant reduction in viability when cells were treated for 24–72 h with N54 at 100 μM or N20 and N43 at 10 μM.

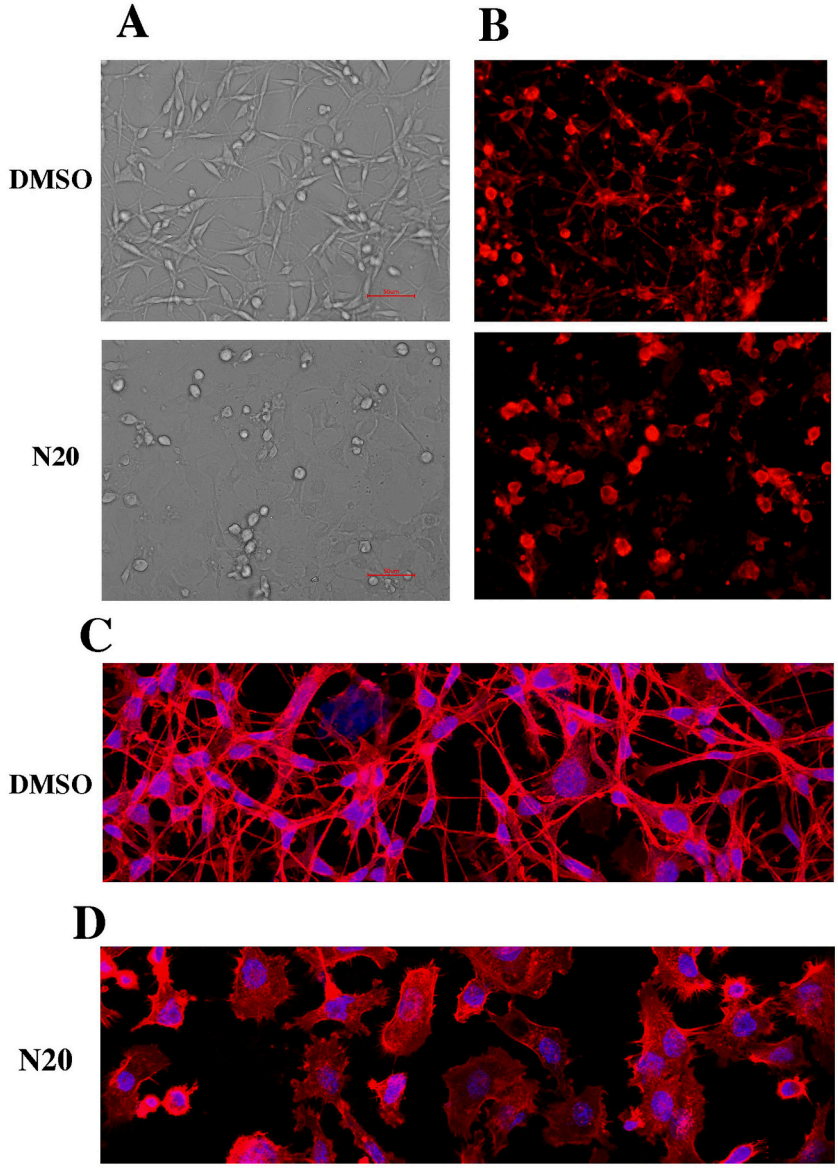

Fig. 4. Analysis of effects of the lead compounds on actin cytoskeleton formation. In (A), the typical spindle-shaped cells for MBA-MB-231 are shown under phase contrast microscopy compared with the more rounded cell morphology in cells treated with N20. Scale bar = 50 μm. Fluorescent imaging of F-actin distribution in treated and control cells is shown in (B) where, at higher resolution (C), the extensive actin fiber network can be seen in the DMSO-treated cells, which is lost in the N20-treated cells (D).

3.3. Effect of lead compounds on migration and invasion

The WCA measures the ability of cells to move randomly into the vacant space created in the cell monolayer, which is related to the reorganization of the cell membrane dynamics through actin cytoskeleton reorganization, a mechanism influenced by WASF3 [6]. This assay typically correlates well between migration, invasion, and metastasis assays. To better understand the lead compounds' ability to prevent three-dimensional migration through membrane pores, we used a standard transwell assay. Although MDA-MB-231 cells are frequently used in invasion assays to assess the effect of WASF3 on invasion and metastasis, we also included Du145 prostate cancer cells in these assays since they are also sensitive to modulation of WASF3 expression [10]. As shown in Fig. 3, the lead compounds could suppress the motility and migration of both cell lines. Since invasion truly reflects the metastatic potential of cancer cells, we also used matrigel-coated inserts in conventional transwell assays. The matrigel inserts in the transwell chambers challenge the cells to pass through a matrix similar to the basement membrane. Consistently, cell invasion was suppressed by the lead compounds in both cell lines. In all three of these in vitro assays, N20 consistently showed the most profound effect.

3.4. Epithelial to mesenchyme transition

One of the consequences of the inactivation of the WASF3 gene in multiple studies has been the change in morphology in the targeted cells characteristic of the epithelial to mesenchyme transition (EMT). In our previous studies manipulating the genetic consequences of WASF3 function, loss of cell motility and invasion is typically accompanied by morphological alteration of cell shape, which is accompanied by altered levels of actin polymerization, which manifests in a decrease in the formation of actin microfilaments and cellular protrusions such as lamellipodia which are responsible for cell movement [26]. Phase contrast images (Fig. 4A) show a typical normal spindle cell appearance in DMSO-treated MDA-MB-231 cells, which are lost when treated with N20. The rounded mesenchymal-like appearance is similar to the effects on cell shape seen when WASF3 is knocked down [10,26]. As shown in Fig. 4B–D, cells treated with N20 show reduced levels of filamentous actin formation compared with DMSO-treated cells, which show extensive formation of interconnecting cell protrusions.

3.5. Analysis of metastasis in a zebrafish model

We have previously reported [23,27] that zebrafish can be used as a convenient and relatively rapid means of assessing the metastatic potential of human cancer cells. Zebrafish embryos do not develop an immune system until ~10 days post fertilization, and during this period, it is possible to maintain human cells in the fish and monitor invasion and dissemination in the transparent zebrafish embryos using confocal microscopy. We used the three lead compounds that showed the most significant suppression of motility in vitro in this zebrafish assay. Compounds were first introduced into the fish water to evaluate the maximum tolerated dose on fish

Drug	Maximum Tolerated Dose (uM)	Effect on Metastasis (Percent embryos showing Metastasis)
DMSO Control	50	60
N20	2	25
N43	50	40
N54	50	45

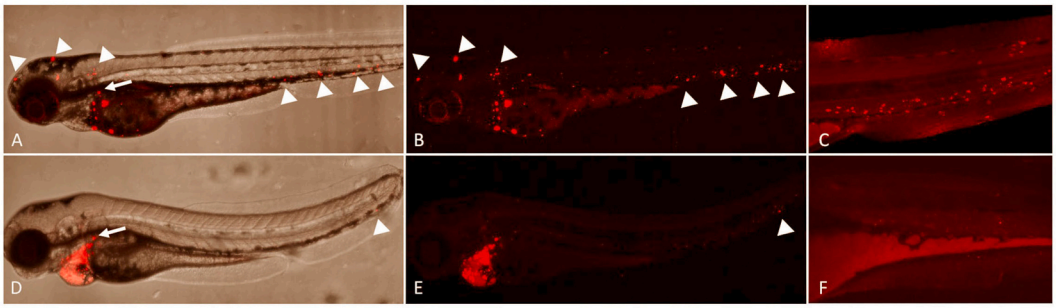

Fig. 5. Zebrafish metastasis assays. Summary of the maximum tolerated dose (MTD) for the lead compounds affecting cell invasion (above). Zebrafish metastasis assays, showing confocal images (below) demonstrating dissemination of individual cells throughout the vasculature of the fish (arrows) following treatment with N20 after 36–48 h. In the DMSO-treated embryos (A), dark field analysis shows the extensive dissemination in the fish body of breast cancer cells labeled with CM-DiI. Fluorescent images (B) show the density of metastasized cells. A higher magnification of the trunk of the fish is shown in (C). In fish treated with N20 (D), the number of disseminated cells is greatly reduced, with only a single cell detected (E) as shown in the expanded view of the fish trunk (F).

embryos using 1, 2, 5, 10, 25, and 50 μM final concentrations (Fig. 5). Embryos were treated from 24 h post fertilization (hpf) until 120 hpf, and the maximum tolerated doses (MTD) and extent of metastasis for the fish cohorts treated with the lead compound were analyzed. MTD was calculated as the concentration at which <10 % showed either deformity or mortality at 120 hpf. To evaluate the effects on metastasis, MDA-MB-231 cells were labeled with the CM-DiI fluorescent dye as described previously [23], and ~200 cells were injected into the perivitelline space of 36–48 hpf embryos, which were then incubated for 36–48 h with the compounds at their MTD and then imaged using confocal microscopy and the presence of metastatic cells in the body of the fish observed. Metastasis was evaluated by determining the number of fish in which at least ten cells were seen in the zebrafish body away from the injection site. When treated with 2 μM, at the lowest concentration, DMSO (n = 89), significant metastasis was seen in over 60 % of embryos. Treatment with N43 and N54 showed only a minor decrease in the percentage of embryos showing metastases (Fig. 5). In contrast, following treatment with N20 (n = 64), only 23 % of embryos showed metastases. These data further reinforce N20 as the most effective compound in our series across the in vitro and in vivo analyses and became the lead compound for further analysis.

3.6. Cellular thermal shift assays

The in vitro and in vivo analysis shows evidence that the lead compounds affect cell invasion and metastasis, and the in silico docking study implies that they bind to WASF3. However, in the absence of a molecular modification, it can sometimes be challenging to demonstrate direct interaction with the target using surrogate analyses. Extensive studies have shown, however, that a ligand binding to its target can perturb protein thermal stability as detected by melting temperature shifts. This principle has been adapted to studies in the normal physiological environment of the cell [24] using the cellular thermal shift assay (CETSA). In this approach, cells are treated with the compound, and then lysates are used to measure the melting profile of the target protein, which is determined by Western blotting across a temperature gradient. MDA-MB-231 and Du145 cells were treated with 10 μM N20 and subjected to temperature changes in two-degree Celsius intervals (Fig. 6). The stability of the WASF3 protein is progressively reduced with increasing temperature and is lost at 60–62° compared with cells treated with DMSO alone. These data suggest that N20 indeed binds to WASF3.

4. Discussion and conclusion

Since WASF3 significantly regulates phenotypes involved in cell invasion, it might be a rational target to suppress metastasis, a

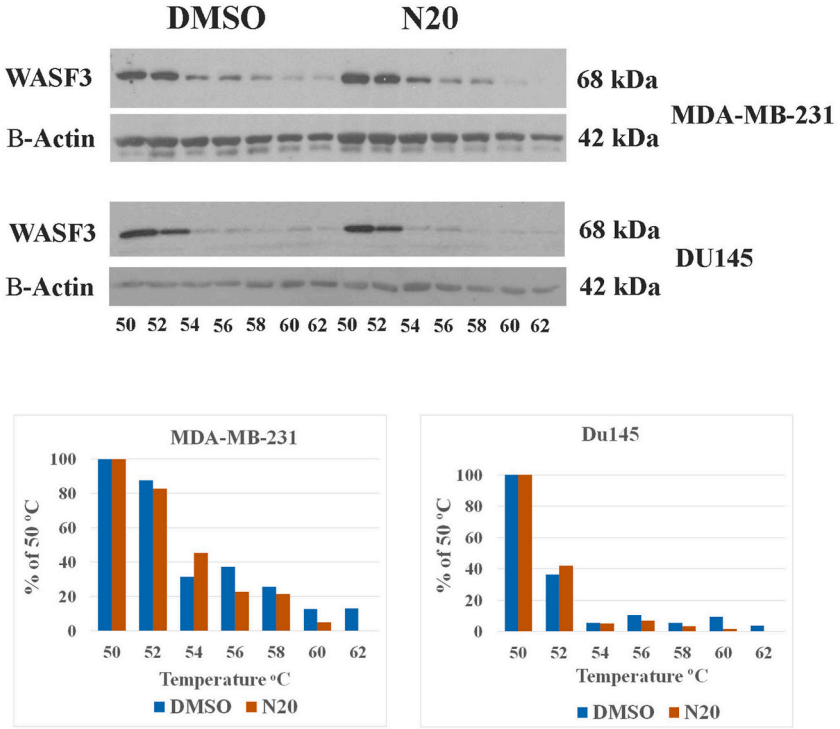

Fig. 6. Cellular thermal shift assays. Equal volumes of cellular protein from MDA-MB-231 cells treated with either DMSO or N20 were analyzed for WASF3 expression levels following denaturation with increasing temperature at 2 °C intervals. Similarly, the thermal stability of WASF3 was determined in Du145 prostate cancer cells. Actin levels in each aliquot was also assayed as a loading control (Above). Densitometric analysis of the protein levels at each temperature was determined using ImageJ, and the relative levels for each temperature between the DMSO and N20 cells were calculated (Below). A progressive reduction in protein stability relative to increasing temperature is seen in both breast and prostate cancer cell lines treated with N20.

contention supported by the observation that stapled peptide disruption of the WASF3 regulatory complex suppresses metastasis [11,12]. Here we report the first identification of a series of small molecules that might achieve the same effect. The only other suggestion of an inhibitory molecule that might affect actin polymerization directed by the closely related WASP proteins came from a study in Xenopus embryos that suggested a small peptide, I187, could suppress activation of the ARP2/3 complex by the closely related *N*-WASP protein [28]. In our unpublished observations, I187 also suppresses invasion in WASF3-expressing breast cancer cell lines. This peptide was also directed against the activation pocket in the WASP/WASF proteins, but since it represents a conventional approach with limitations in targeting efficiency, cell penetration, and stability, it is likely to be less successful than small molecule inhibitors. The consistent demonstration that N20 can suppress invasion and metastasis provides a basis for using medicinal chemistry approaches to develop means to suppress WASF3-directed metastasis. The in vitro invasion assays used in this study have consistently correlated with metastasis in vivo in mouse models [10,29]. In vivo assays represent a more complex view of the ability of specific compounds to effectively suppress the invasion phenotype over and above what can be determined in in vitro cell studies. While metastasis in mice is typically the preferred preclinical foundation approach, the zebrafish model of metastasis is rapidly emerging as a convenient surrogate [23]. Zebrafish have all the characteristics of organ function and plasma involvement. However, they offer the advantage that metastasis of single cells can be monitored in live animals and in real time using confocal microscopy. In addition, these assays can be completed in several days compared with the need for tumor development in mice, which can take months and typically requires the sacrifice of the animals to assess metastasis [10,29]. The close parallel between the metastatic ability of human cells in zebrafish and in vitro characteristics has been demonstrated [23]. The fish, however, report more significant effects of drug toxicity due to affects on metabolism and organ function not seen in cultured cells. This is reflected in the fact that the most active compounds in vitro (N20) are not tolerated in fish assays to the same extent as the other compounds. Although zebrafish are transparent, allowing the visualization of metastatic cells, quantitation is complicated since the fluorescence signal deep in the body can be suppressed. For this reason, instead of absolute numbers of disseminated cells, we used frequency of metastasis, which has been generally adopted for these assays. Demonstrating a direct interaction between a ligand and its target has traditionally been difficult and can frequently lead to compound failure in clinical trials [30]. The CETSA approach, however, has become a trusted means to demonstrate interactions between compounds and protein targets, where the stability of the protein is affected as a result of these interactions [24,31]. Two outcomes have been described, the first where the protein is stabilized due to interaction and the second where the protein is destabilized. Detailed mathematical modeling has demonstrated that the stabilizing effects are due to the compounds binding to the fully folded active protein, and the destabilizing effects are due to binding to the unfolded inactive protein [32]. It appears that N20 destabilizes binding to WASF3 and, therefore, would be predicted to bind the unfolded protein to affect its function. While in silico docking has been successful on many occasions in defining lead compounds in a variety of situations, it is also true that the predictions can be inaccurate for various reasons, such as the state of conformational flexibility upon binding, size of the grid to represent the protein, and difficulties in predicting large complexes [33]. However, we have shown that despite these limitations, we were able to identify candidate compounds that clearly affect invasion and metastasis in model systems. The complication in most of these studies lies in the ability to determine cause and effect. Our premise was that docking to the WASF3 pocket would interfere with its function, although we have been unable to demonstrate an effect on protein complex stability seen when the complex members are disrupted genetically, for example [11,12]. The compromised function of WASF3 as a result of treatment with the macrocyclic compounds, however, is suggested through a correlation with cell movement/invasion and with the effects on actin organization, which is typical of genetic approaches that suppress WASF3 function [6,10,26]. The main characterized functions of WASF3, however, are still limited to its control of actin reorganization through the VCA domain [16] and the ability to direct specific kinase activation and function [5,6,34]. It is clear, though, that beyond the ability of WASF3 to regulate a series of pathways that are related to metastasis, albeit as a result of ablation of the proteins involved [11,12], this does not seem to be the case for N20 since, in CETSA studies, the stability of the protein in treated cells is unaffected. In our study using co-immunoprecipitation and mass spectroscopy studies of WASF3 binding partners, however [35], over 600 proteins were identified as potential interactors, so it is likely that many functional relationships for WASF3 remain to be discovered. Indeed, we have shown that multiple kinases interact with the WASF3 scaffold structure [5,6,34], and it has been predicted that these may be transported to sites of active actin polymerization seen when WASF3 cells [6] are stimulated to migrate. WASF3 has also been shown to interact with mitochondrial proteins as well as Golgi complex proteins [29] and is stabilized through interactions with heat shock proteins [35]. WASF3 also interacts with various membrane-bound receptors, such as members of the ERBB family [8], which is an important intermediate for mutant RAS-induced invasion and metastasis [36]. Unfortunately, while the mode of action of N20 has not been extensively reported, it is included in two US patents [37,38] and is implicated in binding to connexins 30 and 43 and the hepatitis C viral (HCV) structural E2 protein, although there is limited confirmatory evidence beyond this. It is perhaps relevant that connexin-43 has been implicated in cell invasion [39,40], and, while beyond the scope of this study, if it were to interact with WASF3, then this might suggest a potential role for the disruptive influence of N20. Similarly, the HPV E2 protein is also implicated in cell invasion and metastasis [41], possibly through its regulation of MMP9 [42], which is a mediator of WASI3-induced invasion and metastasis [26]. The data in this study suggest that these small compounds inhibit cell motility, migration, and invasion, with N20 being the most potent; therefore, it has the potential to be used as a precursor compound for further directions on the development of anti-metastatic drugs for cancer therapy.

Ethics Approval and Consent to Participate

Not Applicable.

Human and animal right

Not Applicable.

Consent for Publication

Not Applicable.

Availability of data and materials

Data included in article/supp. material/referenced in article.

Funding

This research received no external funding.

CRediT authorship contribution statement

Jeane Silva: Formal analysis, Methodology, Supervision, Visualization, Writing – original draft, Writing – review & editing. **Nivin Omar:** Formal analysis, Methodology, Visualization. **Vinoth Sittaramane:** Formal analysis, Visualization. **John K. Cowell:** Conceptualization, Supervision, Writing – original draft, Writing – review & editing.

Declaration of competing interest

The authors declare that they have no known competing financial interests or personal relationships that could have appeared to influence the work reported in this paper.

Acknowledgements

We are grateful to Dr. A Bahassan for assistance with the early screening protocol, Dr. Thomas Albers for performing the docking analysis, Dr. Iryna Lebedeva for helpful discussions, and Brittney Ikuesan for technical assistance. We also thank the Drug Synthesis and Chemistry Branch, Developmental Therapeutics Program, Division of Cancer Treatment and Diagnosis, National Cancer Institute for providing the compounds used in this study.

Appendix A. Supplementary data

Supplementary data to this article can be found online at https://doi.org/10.1016/j.heliyon.2023.e20662.

List Of Abbreviations

VCA – verprolin-cofilin-acidic
WRC – WASP regulatory complex
PDB – Protein database
DMSO – dimethyl sulfoxide
PBS – phosphate-buffered saline
WCA – wound closure assay
EMT - epithelial to mesenchyme transition
MTD – maximum tolerated dose
CETSA – cellular thermal shift assay
HCV – hepatitis C virus
WIRS – WRC interacting receptor sequence
FBS – fetal bovine serum

References

[1] D.X. Nguyen, J. Massagué, Genetic determinants of cancer metastasis, Nat. Rev. Genet. 8 (2007) 341–352.
[2] G. Jinesh, A.S. Brohl, The genetic script of metastasis, Biol. Rev. 95 (2020) 244–266.
[3] K. Sossey-Alaoui, G. Su, E. Malaj, B. Roe, J.K. Cowell, *WAVE3*, an actin-polymerization gene, is truncated and inactivated as a result of a constitutional t(1;13)(q21;q12) chromosome translocation in a patient with ganglioneuroblastoma, Oncogene 21 (2002) 5967–5974.

[4] K. Sossey-Alaoui, K. Head, N. Nowak, J.K. Cowell, Characterization of the genomic organization and expresssion profile of the human and mouse WAVE gene family, Mamm. Genome 14 (2003) 314–322.
[5] Y. Teng, P. Ghoshal, L. Ngoka, Y. Mei, J.K. Cowell, Critical role of the WASF3 gene in JAK2/STAT3 regulation of cancer cell invasion, Carcinogenesis 34 (2013) 1994–1999.
[6] K. Sossey-Alaoui, X. Li, T.A. Ranalli, J.K. Cowell, WAVE-3 mediated cell migration and lamellipodia formation are regulated downstream of P13-kinase, J. Biol. Chem. 280 (2005) 21748–21755.
[7] P. Ghoshal, Y. Teng, L. Lesoon, J.K. Cowell, HIF1A induces expression of the WASF3 Metastasis Associated Gene under hypoxic conditions, Int. J. Cancer 131 (2012) E905–E915.
[8] Y. Teng, W. Pi, Y. Wang, J.K. Cowell, WASF3 provides the conduit to facilitate invasion and metastasis in breast cancer cells through HER2/HER3 signaling, Oncogene 35 (2016) 4633–4640.
[9] K. Sossey-Alaoui, A. Safina, X. Li, M.M. Vaughan, D.G. Hicks, A.V. Bakin, J.K. Cowell, Down-regulation of WAVE3, a metastasis promoter gene, inhibits invasion and metastasis of breast cancer cells, Am. J. Pathol. 170 (2007) 2112–2121.
[10] Y. Teng, M. Ren, R. Cheney, S. Sharma, J.K. Cowell, Inactivation of the WASF3 gene in prostate cancer cells leads to suppression of tumorigenicity and metastases, Br. J. Cancer 103 (2010) 1066–1075.
[11] Y. Teng, H. Qin, A. Bahassan, N.G. Bendzunas, E.J. Kennedy, J.K. Cowell, The WASF3-NCKAP1-CYFIP1 complex is essential for breast cancer metastasis, Cancer Res. 76 (2010) 5133–5142.
[12] Y. Teng, A. Bahassan, D. Dong, L.E. Hanold, X. Ren, E.J. Kennedy, J.K. Cowell, Targeting the WASF3-CYFIP1 complex using stapled peptides suppresses cancer cell invasion, Cancer Res. 76 (2016) 965–973.
[13] J.K. Cowell, Y. Teng, N.G. Bendzunas, R. Ara, A.S. Arbab, E.J. Kennedy, Suppression of breast cancer metastasis using stapled peptides targeting the WASF regulatory complex, Cancer Growth Metastasis 10 (2017) 1–9.
[14] C.F. Stovold, T.H. Millard, L.M. Machesky, Inclusion of scar/WAVE3 in a similar complex to scar/WAVE1 and 2, BMC Cell Biol. 6 (2005) 11.
[15] S. Eden, R. Rohatgi, A.V. Podtelejnikov, M. Mann, M.W. Kirschner, Mechanism of regulation of WAVE1-induced actin nucleation by Rac1 and Nck, Nature 418 (2002) 790–793.
[16] T. Takenawa, S. Suetsugu, The WASP-WAVE protein network connecting the membrane to the cytoskeleton, Nat. Rev. Mol. Cell Biol. 8 (2007) 37–48.
[17] B. Chen, Z. Chen, K. Brinkmann, C.W. Pak, Y. Liao, S. Shi, L. Henry, N.V. Grishin, S. Bogdan, M.K. Rosen, Structure and control of the actin regulatory WAVE complex, Nature 468 (2010) 533–538.
[18] Z. Chen, D. Borek, S.B. Padrick, T.S. Gomez, Z. Metlagel, A. Ismail, J. Umetani, D.D. Billadeau, Z. Otwinowski, M.K. Rosen, The WAVE regulatory complex links diverse receptors to the actin cytoskeleton, Cell 156 (2014) 195–207.
[19] N.P. Coussens, J.C. Braisted, T. Peryea, G.S. Sittampalam, A. Simeonov, M.D. Hall, Small-molecule screens: a gateway to cancer therapeutic agents with case studies of food and drug administration-approved drugs, Pharmacol. Rev. 69 (2017) 479–496.
[20] L. Pinzi, G. Rastelli, Molecular docking: shifting paradigms in drug discovery, Int. J. Mol. Sci. 20 (2019) 4331.
[21] N.M. O'Boyle, M. Banck, C.A. James, C. Morley, T. Vandermeersch, G.R. Hutchison, Open Babel: an open chemical toolbox, J. Chemoinformat 3 (2013) 33.
[22] O. Trott, A.J. Olson, AutoDock Vina: improving the speed and accuracy of docking with a new scoring function, efficient optimization, and multithreading, J. Comput. Chem. 31 (2010) 455–461.
[23] Y. Teng, X. Xie, S. Walker, M. Saxena, D. Kozlowski, J. Mumm, J.K. Cowell, Evaluating human cancer cell metastasis in zebrafish, BMC Cancer 13 (2013) 453.
[24] R. Jafari, H. Almqvist, H. Axelsson, M. Ignatushchenko, T. Lundbäck, P. Nordlund, D.M. Molina, The cellular thermal shift assay for evaluating drug target interactions in cells, Nat. Protoc. 9 (2014) 2100–2122.
[25] A. Zweifach, The national cancer institute's plated compound sets can Be a valuable resource for academic researchers, SLAS Discov 25 (2020) 2–6.
[26] K. Sossey-Alaoui, T.A. Ranalli, X. Li, A.V. Bakin, J.K. Cowell, WAVE3 promotes cell motility and invasion through the regulation of MMP-1, MMP-3, and MMP-9 expression, Exp. Cell Res. 308 (2005) 135–145.
[27] J. Shao, Y. Teng, R. Padia, S. Hong, H. Noh, X. Xie, J.S. Mumm, Z. Dong, H.-F. Ding, J.K. Cowell, J. Kim, J. Han, S. Huang, COP1 and GSK3β cooperate to promote c-Jun degradation and inhibit breast cancer cell metastasis, Neoplasia 15 (2013) 1075–1085.
[28] J.R. Peterson, R.S. Lokey, T.J. Mitchison, M.W. Kirschner, A chemical inhibitor of N-WASP reveals a new mechanism for targeting protein interactions, Proc Natl Acad Sci 98 (2001) 10624–10629.
[29] Y. Teng, X. Ren, H. Li, A. Shull, J. Kim, J.K. Cowell, Mitochondrial ATAD3A combines with GRP78 to regulate the WASF3 metastasis-promoting protein, Oncogene 35 (2016) 333–343.
[30] D. Martinez Molina, R. Jafari, M. Ignatushchenko, T. Seki, E.A. Larsson, C. Dan, L. Sreekumar, Y. Cao, P. Nordlund, Monitoring drug target engagement in cells and tissues using the cellular thermal shift assay, Science 341 (2013) 84–87.
[31] T.T. Waldron, K.P. Murphy, Stabilization of proteins by ligand binding: application to drug screening and determination of unfolding energetics, Biochemistry 42 (2003) 5058–5064.
[32] P. Cimmperman, L. Baranauskiene, S. Jachimoviciūte, J. Jachno, J. Torresan, V. Michailoviene, J. Matuliene, J. Sereikaite, V. Bumelis, D. Matulis, A quantitative model of thermal stabilization and destabilization of proteins by ligands, Biophys. J. 95 (2008) 3222–3231.
[33] C. Pons, S. Grosdidier, A. Solernou, L. Pérez-Cano, J. Fernández-Recio, Present and future challenges and limitations in protein-protein docking, Proteins 78 (2010) 95–108.
[34] K. Sossey-Alaoui, X. Li, J.K. Cowell, c-ABL-mediated phosphorylation of WAVE3 is required for lamellipodia formation and cell migration, J. Biol. Chem. 82 (2007) 26257–26265.
[35] Y. Teng, L. Ngoka, Y. Mei, L. Lesoon, J.K. Cowell, HSP90 and HSP70 are essential for stabilization and activation of the WASF3 metastasis promoting protein, J. Biol. Chem. 287 (2012) 10051–10059.
[36] Y. Teng, L. Ngoka, J.K. Cowell, Promotion of invasion by mutant RAS is dependent on activation of the WASF3 metastasis promoter gene, Genes Chroms. Cancer 56 (2017) 493–500.
[37] Us patent Us9879058, Use of compounds that selectively modulate astrocytic release of substances through hemichannels of connexins and pannexins, without influencing gap junctions, for the treatment of psychiatric disorders (2018).
[38] Us patent Us2016361311, Ligands that Target Hepatitis C Virus E2 Protein, 2015.
[39] T. Aasen, E. Leithe, S.V. Graham, P. Kameritsch, M.D. Mayán, M. Mesnil, K. Pogoda, A. Tabernero, Connexins in cancer: bridging the gap to the clinic, Oncogene 38 (2019) 4429–4451.
[40] J. Wu, L. Wang, Emerging roles of gap junction proteins connexins in cancer metastasis, chemoresistance and clinical application, J. Biomed. Sci. 26 (2019) 8.
[41] M. Muller, C. Demere, The HPV E2-host protein-protein interactions: a complex hijacking of the cellular network, Open Virol. J. 6 (2012) 173–189.
[42] B. Akgül, R. García-Escudero, C. Ekechi, G. Steger, H. Navsaria, H. Pfister, A. Storey, The E2 protein of human papillomavirus type 8 increases the expression of matrix metalloproteinase-9 in human keratinocytes and organotypic skin cultures, Med. Microbiol. Immuno. 200 (2001) 127–135.